energies

MDPI

Article

Hydrogen Vortex Flow Impact on the Catalytic Wall

Vadim Lemanov, Vladimir Lukashov * and Konstantin Sharov

Kutateladze Institute of Thermophysics Siberian Branch of RAS, 630090 Novosibirsk, Russia
* Correspondence: luka@itp.nsc.ru

Abstract: An experimental study of a hydrogen-containing jet's impact on a palladium-based catalyst in an air atmosphere was carried out. High-intensity temperature fluctuations on the catalyst surface are obtained in the case when large-scale vortex structures are contained in the jet. These superstructures have a longitudinal size of 20–30 initial jet diameters and a transverse size of about 3–4 diameters. To form such structures, it is necessary to use long, round tubes in the Reynolds number range of 2000–3000 as a source of the impinging jet when a laminar-turbulent transition occurs in the channel according to the intermittency scenario. This effect was obtained at a low hydrogen content in the mixture (X_{H2} = 3 ... 15%) and a low initial temperature of the catalyst (180 °C). It is shown that the smallest temperature fluctuations are obtained for the laminar flow in the tube (<1.5%), and they are more significant (<4%) for the turbulent regime at low Reynolds numbers (Re < 6000). The greatest temperature fluctuations were obtained during the laminar-turbulent transition in the tube (up to 11%). Two important modes have been established: the first with maximum temperature fluctuations in the local region of the stagnation point, and the second with the greatest integral increase in temperature fluctuations over the entire area of the catalyst.

Keywords: impinging jet; large vortex structure (puff); catalysis; hydrogen

Citation: Lemanov, V.; Lukashov, V.; Sharov, K. Hydrogen Vortex Flow Impact on the Catalytic Wall. *Energies* **2023**, *16*, 104. https://doi.org/10.3390/en16010104

Academic Editor: Bjørn H. Hjertager

Received: 29 October 2022
Revised: 14 December 2022
Accepted: 19 December 2022
Published: 22 December 2022

1. Introduction

Catalytic surfaces are widely used in modern technological processes and in the power industry. These include, for example, catalytically assisted combustion [1,2] and heterogeneous catalytic processes used for heating [3,4]. Impinging jets can be attributed to one of the most common reactor geometries. With this arrangement of flows, the fuel mixture jet flows out of the nozzle, hole or tube and interacts with a flat or spatial obstacle. An example is the use of impinging jets in gas burners [5], in mixers [6,7] and in chemical reactors [8,9]. Estimates of the influence of flow dynamics on the features of kinetics of catalytic hydrogen oxidation move in the first place when analyzing the passive protection systems of nuclear power plants [10]. The optimization of heat and mass transfer during the inflow of an impinging reagents mixture onto an obstacle and the heterogeneous oxidation of gaseous fuel on a substrate is one of the most important tasks for organizing the efficient deposition of functional coatings from precursor vapors in CVD processes [11].

From the point of view of fundamental science, the various gases' interaction with catalysts is currently being studied at the interaction level of gas phase molecules with elements of the crystal lattice of the catalyst solid phase. Great progress has been achieved in this direction. In particular, such phenomena as bistability, surface wave, spatiotemporal chaos, pattern, chemical turbulence and others are studied [12,13]. Such complex processes are studied, as a rule, under the conditions of ultrahigh vacuum, when gases with a high purity composition are used, and single crystals of metals are used as a catalytic surface [14]. It is quite difficult to transfer the achievements made at the molecular level to the macroscales typical of practice; this is the so-called "pressure and materials gap" problem [15]. In this regard, in practice, along with numerical modeling, experimental data and correlations obtained as a result of their generalization are of great importance for combustion and heat and mass transfer processes.

It is known that in the presence of a catalyst, the temperature of fuel ignition decreases. This advantage allows the combustion of extremely lean mixtures. Precious metals such as platinum and palladium are often used for these purposes. As it is known from the literature on catalytic combustion, there are various regimes of such device operation. Thus, in [16], in a numerical simulation of the homogeneous jet flow of air with hydrogen onto a catalytic barrier, four regimes were determined: (1) only surface reaction; (2) surface reaction inhibiting homogeneous reaction; (3) homogeneous reaction inhibiting surface reaction; and (4) only homogeneous reaction. These regimes depend significantly on the plate temperature, on the strain rate in the near-wall boundary layer and on the composition and temperature of the reagent flow. At relatively low surface temperatures and low hydrogen concentrations in the external flow, heterogeneous reactions predominate, while at higher temperatures and higher concentrations, homogeneous reactions predominate. Heat transfer and chemical reactions in hydrogen-air mixtures falling normally on a hot platinum-coated plate were calculated numerically in [17]. Chemical reactions take place both in the gas phase and in the platinum layer. It is shown that the production of rare compounds such as OH and O is negligible, although they may be the major contributors. New correlations for the global reaction rate of H_2 with O_2 and the Sherwood number versus Reynolds number were obtained for *Re* ranging from 58 to 2315. As the Reynolds number increases, the Sherwood number and the surface reaction rate increase almost linearly.

There are a limited number of publications dealing with the experimental study of the interaction of a reacting impinging jet with a catalytic surface. One of the first such works was [18], a study of homogeneous and heterogeneous air oxidation reactions of NH_3, CH_4 and C_3H_8 over the heated platinum foil in an atmospheric pressure flow reactor depending on the flow rate, fuel concentration, preheating temperature and reactor geometry. Heterogeneous ignition occurred at about 600 °C for CH_4 and 200 °C for all other systems and was weakly dependent on the fuel composition. The second heterogeneous ignition occurred during oxidation at a temperature ranging from 400 °C to 600 °C.

In the experiment of [19], the combustion of hydrogen and air mixtures on the surface of platinum foil was considered, and diagnostic access for thermocouples and sampling probes was also obtained to measure the profiles of the boundary layer of the gas phase. Similar measurements in the near-wall boundary layer were made in [20]. This paper focuses on the strontium-palladium catalyst material, which shows very good low-temperature activity, with the catalyst powder converting 1/2 of the fuel at T = 406 °C. In [9], an impinging jet reactor was used to evaluate the kinetics of H_2/O_2 reactions on Rh/Al_2O_3 catalysts. The experiments on H_2 oxidation were carried out at various fuel/oxygen ratios and temperatures. Using experimental data obtained at relatively high temperatures, a new kinetic dataset for 12-step mechanisms of H_2 oxidation was presented. Sensitivity analysis showed that the steps of hydrogen adsorption and desorption are the key stages, and the mechanism is very sensitive to gas-phase H_2O, adsorbed H_2O and OH particles.

Thus, it can be concluded that, despite the widespread use of catalytically active surfaces in technological processes, there are relatively few works on the influence of heat and mass transfer of the features of the interaction of reacting flows with catalytic surfaces.

At present, the method of controlling the combustion processes of a gaseous fuel jet using large-scale turbulent structures is widely used [21,22]. The term "Large Scale Structures" was first used in relation to large eddies with a size (l = 3–5 δ) in near-wall and free streams in the 70-th [23–25]. Later, the term "Coherent Structures" became more common [26–28]. In recent years, the terms "Very Large Scale Structures" and "Superstructures" have appeared, which refer to eddies with a size (l = 10–20 δ) for inertial flows [29–31]. In particular, for flowing in pipes, it was found that during laminar-turbulent transition, large-scale turbulent eddies (l = 10–20 d) are formed, which are called puff [32–34]. As it is known, the most intense processes of oxidation and combustion are localized in the chemical reaction front [35]. In the presence of convective motion, the process of turbulent diffusion is much more intense than the process of molecular diffusion. According to modern concepts, the fundamental mechanism of turbulent diffusion is the deformation of

microvolumes (compression-tension, shear, rotation) [36]. Typically, this is achieved at the expense of large local velocity gradients, which result in a high level of turbulent energy. In this case, high levels of velocity, temperature and concentration pulsations are observed. The approach using large-scale turbulent structures is just aimed at increasing turbulent energy, which leads to the intensification of heat and mass transfer processes for both inert flows and reacting flows in the front of a chemical reaction [21,37,38]. In this work, modern achievements in the field of laminar-turbulent transition in pipes and jets are used. In our previous studies for inert and reactive jets, it was found that large-scale vortex structures (puffs) flowing out of the tube are stable in the near zone of the jet ($x/d < 15$). These superstructures have a longitudinal dimension $l/d \sim 20$–30 and significantly affect the jet flow [39]. In particular, it was shown that in this way, it is possible to transfer an attached diffusion flame to a detached one and vice versa, change the laminar flow in the flame to turbulent and even carry out flame extinction [40]. In the present work, an experimental study of the interaction of an impact jet of hydrogen with a solid flat surface of a catalyst in the Reynolds number range of 2000–4000 is carried out, when large-scale vortex structures are formed in the impact jet. A jet of fuel mixture of hydrogen and diluent gas flows out of a long tube into the air. In the regime of laminar-turbulent transition, large-scale vortex structures are formed in the tube. These turbulent vortices should lead to a high level of turbulent energy and, accordingly, to the intensification of transport processes in the front of a heterogeneous reaction, that is, on the catalyst surface. The applied orientation of the work dictates to us low concentrations of hydrogen (X_{H2} = 15%) at low temperatures of the preheated catalyst (T_C = 180 °C). The focus of our work is on puff diagnostics and thermal performance on inert and catalytic surfaces.

2. Experimental Setup and Measurement Methods

The main idea of our approach is the use of large-scale turbulent structures for the problem of the interaction of impinging jets reacting with catalytic surfaces. In this regard, our numerous tools (Table 1) were aimed at solving the following problems.

Table 1. Experimental conditions.

№	Test Setup	Working Fluid	*d*, mm/*L*, mm	*h*/*d*	Measuring System	*Re*	Measurements
1	impinging jet	Freon 22	3/1000	10	Schlieren + Hilbert Optic	2600	Visualization
2	free jet	CO_2	8/1600	-	PIV	2400–3100	Velocity fields
3	impinging jet	air	3/1000	20	Film heat flux sensors (HFS)	40–20,000	Local instantaneous heat flux at the stagnation point
4	impinging jet + catalysis	$H_2 + N_2$	3/1000	10	Testo 890-2, FLIR x6530sc	1800–2900	Temperature fields

The first problem has to do with the diagnostics of large-scale structures in free and impinging jets of various gases. In the framework of the first problem: (a) visualization of the flow in an impinging freon jet (F22) using the Schlieren method and Hilbert optics; (b) measurement of the velocity field in a free CO_2 jet using a high-speed PIV. The second problem has to do with the study of the interaction of various gases with inert and catalytic surfaces. The program of the second task included: (a) local measurement of the heat flux at the critical point of the impinging air jet using a film sensor; (b) measuring the temperature on the catalyst surface in an impinging jet of H_2 + Ar, $H_2 + N_2$, H_2 + air using a low-speed (Testo890-2) and high-speed (FLIR x6530sc) thermal imagers.

The main attention in this work is paid to the thermal characteristics of the inert and catalytic surfaces. Such experiments were carried out on the setup shown in Figure 1. Under the conditions considered, the jet flowed out of a long tube (4) into still air and flowed at an angle of 90° onto a plate (2) with a heater (3) with an automatic temperature controller.

The distance from the tube to the obstacle was varied. No artificial perturbations were introduced into the air path of the tube. The gas flow was controlled by a flow meter (1). The surface temperature was measured with a thermal imager (5). The geometric parameters of the working sections, the structure of the optical and other measuring systems, as well as the composition of the working gases in each series of experiments are given in Table 1. The Reynolds number ($Re = Ud/\nu$) was determined from bulk velocity U, tube diameter d and the kinematic viscosity of the fuel mixture ν at room temperature and atmospheric pressure. The viscosity of mixture was determined from the reference data [41].

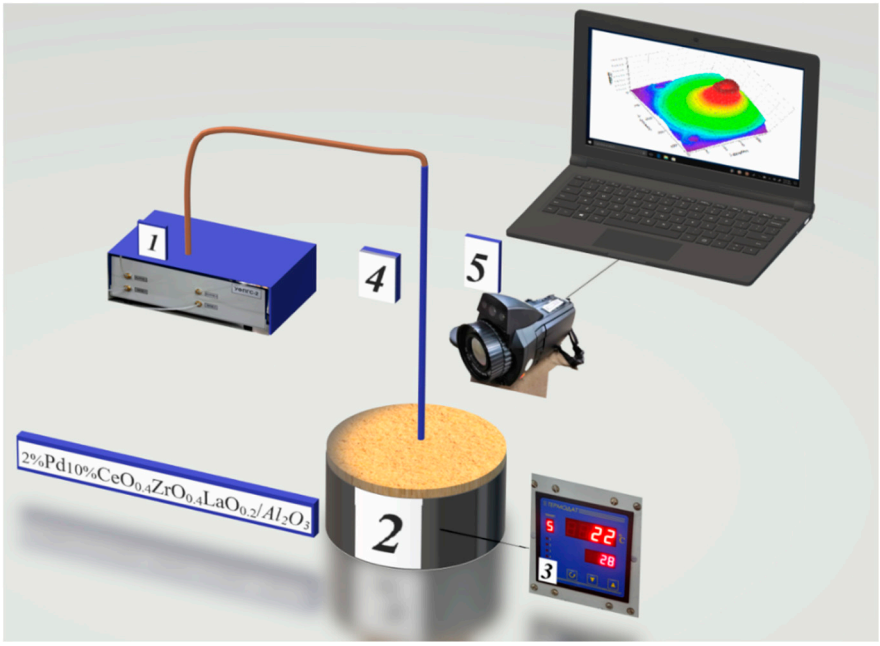

Figure 1. The scheme of experiment with the catalytic surface. 1—gas flow controller; 2—catalytic surface; 3—heater with temperature controller meter; 4—fuel supply pipe; 5—thermal imaging camera.

To study the interaction of a reacting jet flow with an obstacle under the conditions of vortex structure (puff) appearance, we used the reactor shown in Figure 2 for the case of jet movement from bottom to top. The catalyst used to form the coating on the metal disk is gamma alumina modified with rare earth metals and containing palladium as an active catalytic component with the composition of $2\%Pd/10\%CeO_{0.4}ZrO_{0.4}LaO_{0.2}/Al_2O_3$. The catalyst was obtained using the Pechini method (the method of complex ester polymer precursors using an intermediate product of polycondensation of ethylene glycol and citric acid and nitrate salts of metal modifiers) [42]. Systems based on cerium and zirconium dioxides promoted by lanthanum cations have a high mobility of surface and lattice oxygen, which allows their application in the oxidation of various classes of substances, including hydrogen. The deposition of an intermediate layer of TiO_2 and a catalyst on a metal disk was carried out sequentially by the aerosol method described in RF patent 2549619. The presented flow geometry allows the simulation of a surface heterogeneous reaction on the substrate surface under conditions of convective flow around the reagents. In these experiments, mixtures of H_2 + Ar, H_2 + N_2 and H_2 + air were used.

Before starting the process, the temperature of the catalyst-coated surface was brought up to 175 °C using an automatic temperature controller (3). This value was recorded by a thermal imager, and in some experiments, it was additionally controlled by a thermocouple. For the catalytic material used in this work, a stationary process of catalytic heterogeneous combustion of hydrogen was started at this temperature. After that, the thermal power supplied to the ohmic heater was kept constant. During the measurements, the thermal imager recorded the temperature distributions of the catalyst surface shown in Figure 2. As is known from [16], during the catalytic combustion of hydrogen-air mixtures, up to surface

temperatures of 700 °C, the transition of the reaction to the gas phase is not observed. Therefore, we believe that the thermograms measured in this work using a thermal imager correspond to the temperature on the outer surface of the catalyst.

Figure 2. External view of the catalytic reactor.

The main parameter necessary to implement the idea of high-intensity structures interaction of the reacting gas with the catalyst is the temperature field. The temperature distribution on the heated catalyst surface was studied using a FLIR x650sc high-speed thermal imager. This thermal imager is equipped with a matrix based on cadmium-mercury telluride (CMT) crystals with a maximum shooting frequency of 1.5 kHz. The sensor allows the registration of infrared radiation with a wavelength from 1.5 to 5.1 μm. The thermal imager is equipped with GigabitEthernet and CameraLink interfaces. The results of the registration of thermal imaging fields were recorded on the hard disk of a personal computer with subsequent computer processing of the primary data. In that work, the shooting frequency was 100 Hz, and the frame resolution was 320 × 512 pixels. Also, a thermal imaging camera Testo 890-2 with an uncooled microbolometric matrix of 640 × 480 (spectral range of 8–14 μm, measured temperature range from −20 to 1200 °C, sensitivity of 0.08 °C) was used in the work. The temperature measurement uncertainty was ±2%. The frame rate was 9 Hz.

To compare thermal fluctuations obtained for the reacting jet and for the inert jet, the heat flux in the impinging air jet interacting with a flat heated plate was measured. In this experiment, the measurements at the stagnation point were made using a thin-film gradient heat flux sensor (GHFS). The principle of sensor operation is based on the transverse Seebeck effect; in this case, the thermo-EMF is proportional to the temperature gradient and linearly related to the heat flux density [43]. The sensor was installed flush with the surface at the stagnation point of the heated plate, the film thickness was 0.2 mm, and the size of the sensitive part was 2 × 2 mm. The measuring circuit included a GHFS sensor, a preamplifier, an analog-to-digital converter, and a computer. Such a data acquisition system allowed us to obtain the values of heat flux density q with a maximum frequency of up to 3 kHz [43]. According to the time series Q (sample size N = 10,000), mean values and mean square values were determined.

The vortex structures of the puff type in a free jet were detected using high-speed PIV; the outflow occurred into a flow channel made of Plexiglas 400 × 400 × 400 mm in size. An aluminum tube with inner diameter d = 8 mm and length L = 1.6 m (L/d = 200) was used as a jet source. In these experiments, we used CO_2 gas, which flowed into the air under atmospheric conditions. For PIV operation, an aerosol generator was used, in which small droplets of glycerol with a diameter of 3–5 μm were generated. The jet was illuminated with a laser sheet, and the development of puff structures was recorded using a PhotronicsDM high-speed pulsed laser with the help of a PhotronSA5 high-speed camera with a 4-megapixel matrix. Video recording in the experiments was carried out at a frequency of 7 kHz. The resulting images were processed using the PIV technique [44]. As a result, the fields of instantaneous velocities were calculated; using these fields, the

distributions of instantaneous velocities over time on the axis and in the mixing layer of the jet were obtained.

To visualize large-scale vortex structures, experiments on the interaction of an impinging freon (F22) jet with a flat surface without heating were carried out. The use of freon as a working gas is associated with obtaining the most contrasting image of puff structures. In these experiments, an IAB-463M shadow device modified with Hilbert optics was used. The experimental technique and optical characteristics of the device are described in detail in [45]. The video was made with a Canon 650D camera at 50 Hz. A brass tube with inner diameter d = 3 mm and length L = 1 m (L/d = 333) was used as a jet source.

3. Visualization of Large-Scale Structures in an Impinging Jet

In the first stage, large-scale vortex structures were visualized during the interaction of an impinging freon jet (F22) with a flat surface without heating. In these experiments, the shadow method modified with the help of Hilbert optics was used. This technique, using a freon jet propagating in air, allows the creation of significant gradients in refractive indices and obtaining photographs with higher contrast [45]. The inflow of an impinging jet of F22 on the obstacle at h/d = 15 is shown in Figure 3. Three photographs represent a video sequence in the form of three consecutive frames taken at a frequency of 50 Hz. The Reynolds number Re = 2600 corresponds to the regime of laminar-turbulent transition in the jet source for this experiment. The first frame shows the laminar flow in the tube and, accordingly, the laminar flow in the jet. Two different puffs are fixed on the second and third frames. The arrows in Figure 3b,c show the regions where the turbulent vortex structure flowing out of the tube ends and the flow in the jet returns to the laminar regime. It can be seen that a puff is a large-scale turbulent vortex motion in the longitudinal direction. The longitudinal size of the structures was l = 20–30 d, while the distance from the beginning of the jet to the plate h = 15 d. The low shooting speed (50 frames per second) did not allow for the fixing of the dynamics of an individual puff. When a puff interacts with the wall, a strong local deformation occurs in the region of the critical point. As a result, its longitudinal size is reduced, and the superstructure is transformed into smaller vortices that propagate along the wall. The data obtained with a high-speed camera and fixing the internal structure of the puff will be presented below. As shown by our PIV measurements performed in the x/d = 0.3 section, the vortex formations in the free jet are the result of the outflow of large-scale structures formed in the tube.

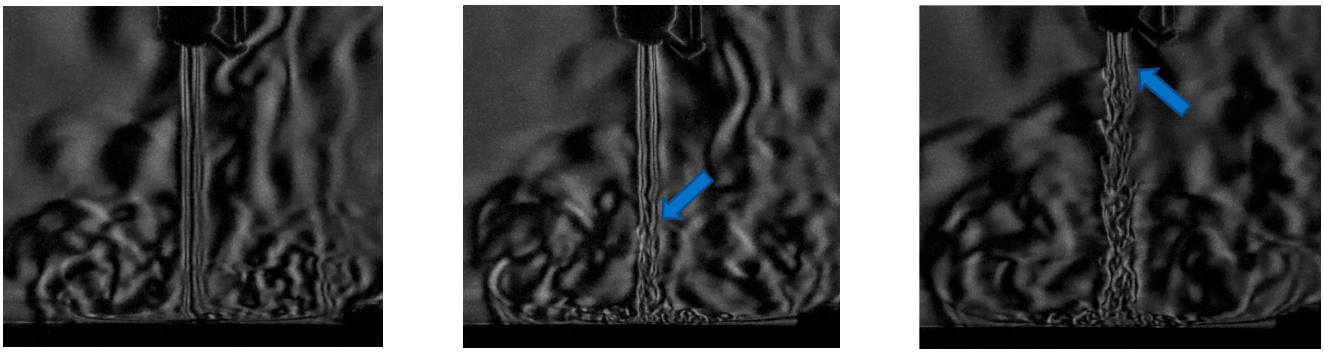

(**a**) (**b**) (**c**)

Figure 3. The flow of Freon-22 jet on the obstacle, isothermal flow, d = 3 mm, flow from top to bottom. Camera Canon EOS 6500, ISO 12800, 1/4000 s. Gilbert diagnostics. (**a**)—unperturbed laminar impinging jet; (**b**,**c**)—the flow of a puff-type vortex structure on the obstacle.

4. The Puff Structure in Free Jet of CO_2

The puff-type vortex structures in a free CO_2 jet were examined using high-speed PIV (shooting frequency of 7 kHz). The distributions of instantaneous longitudinal velocities for a single puff structure over a short time of 1–1.2 s (Re = 2400) are presented in Figure 4.

Three time series are presented for jet section x = 60 mm: on the axis for r = 0 mm (a) and for distances r = 3 mm (b) and r = 4 mm (c) from the axis. The velocity distribution on the axle is characterized by a flat leading edge, while the trailing edge is much steeper, which is a feature of puff structures. It is known that the longitudinal velocity inside turbulent puff structures in a tube decreases in the central part of the channel to ~0.6 *Um* [32]. As can be seen from the figure, the velocity on the jet axis decreases to ~0.25–0.3 *Um*. Comparison of the values of the longitudinal velocity component at r = 0 mm with those at radius r = 3 mm and r = 4 mm reveals short-term correlations at the moment of passage through the turbulent structure. This is illustrated by vertical green lines that correspond to different times t_0–t_5 when the comparison takes place at different radii of the jet flow. Correlation at different radii characterizes the transverse dimension of the puff. On the other hand, the Kelvin-Helmholtz instability in the initial section develops in the mixing layer, and not on the jet axis. An analysis of time series at different distances from the axis shows that the trailing edge in the mixing layer (r = 4 mm) lags slightly behind the similar front on the axis (r = 0). Let us note that the local extremum on the axis (r = 0) does not always correspond to the local extremum at the jet periphery (r = 3–4 mm), for example, for times t_2, t_3 and t_5.

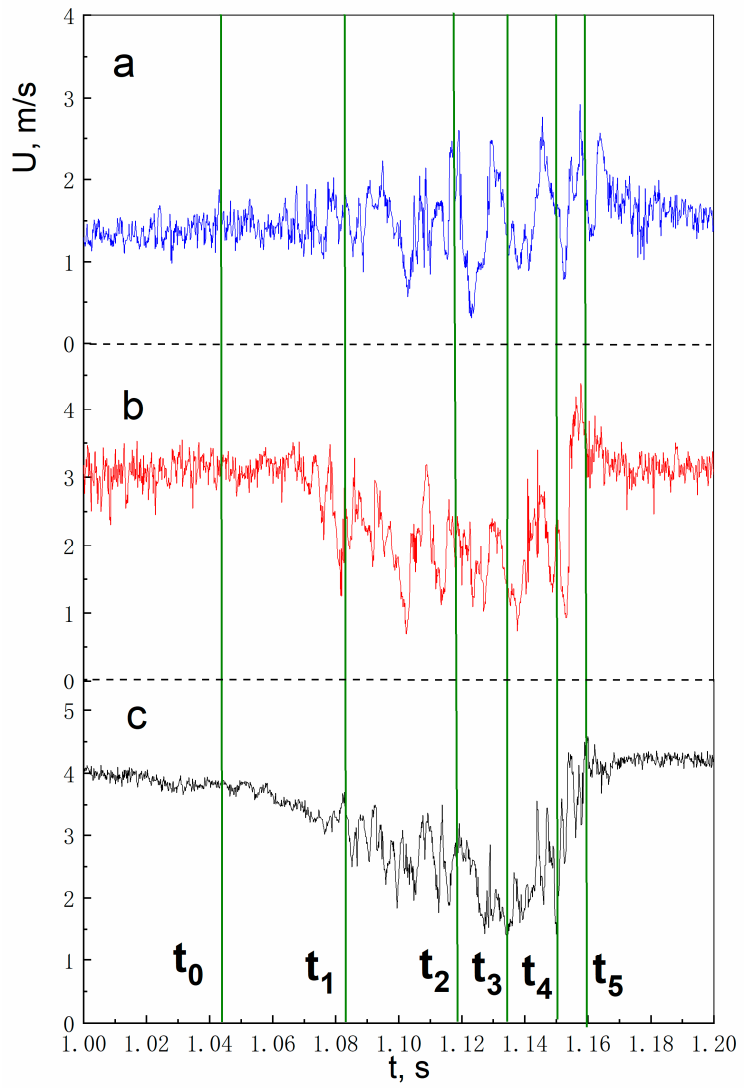

Figure 4. Time series of a single puff velocity in the mixing layer at a distance of r = 4 mm (**a**) and r = 3 mm (**b**) from the axis and on the axis (r = 0) (**c**) in cross-section x = 60 mm (CO_2), *Re* = 2400. t_0 = 1.04 s; t_1 = 1.08 s; t_2 = 1.12 s; t_3 = 1.13 s; t_4 = 1.15 s; t_5 = 1.16 s.

5. Heat Transfer in an Impinging Air Jet

To compare thermal fluctuations obtained for the reacting jet and for the inert jet, the heat flux in the impinging air jet interacting with a flat heated plate was measured. Under the considered conditions, an air jet flowed out of a tube with inner diameter d = 3 mm and length L = 1 m (L/d = 333) into the air and flowed at an angle of 90° onto a heated copper plate 190 mm in diameter and 50 mm thick with wall temperature Tw = const = 47–50 °C. The distance from the tube to the obstacle was set in the range h = 60 mm (h/d = 20). No artificial perturbations were introduced into the air path of the tube. The heat flux measurements at the stagnation point were carried out using a thin-film gradient heat flux sensor (GHFS). The principle of sensor operation and its geometric characteristics are given in the description of the experimental setup.

The heat flux density at the stagnation point of an impinging inert jet is presented in Figure 5 for three versions of initial conditions in the jet. At Re < 3100, a laminar flow with a parabolic velocity profile and a low level of turbulent fluctuations (Tu < 1%) was observed in the initial section of the jet. In the Re = 3100–3700 range, the velocity profile was restructured from the parabolic one to the power law. At Re > 3700, a turbulent flow appeared in the initial section of the jet. Restructuring of the velocity profile indicates that in the region of Reynolds numbers Re = 3100–3700, a laminar-turbulent transition occurs in the tube. In this range, the level of velocity pulsation at the tube outlet increases significantly, and the degree of turbulence reaches the maximum value Tu = 13% at Re = 3320. In this case, the Kelvin-Helmholtz instability develops in the mixing layer of the jet.

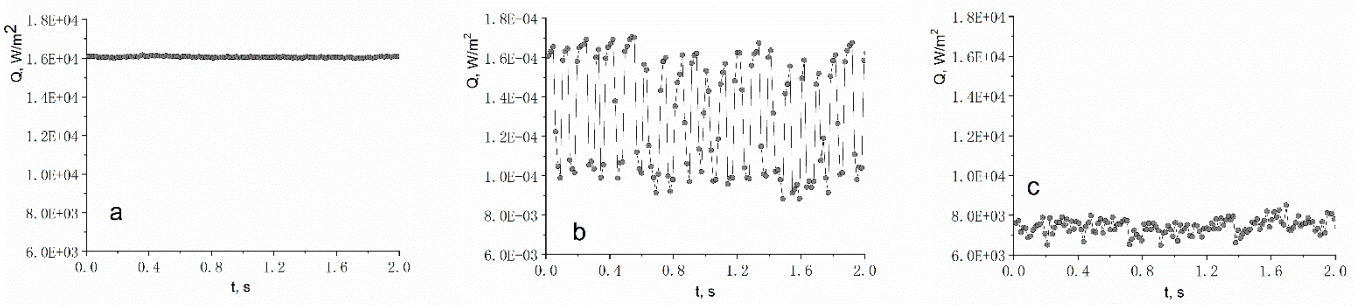

Figure 5. Heat transfer on a flat surface of an impinging inert jet: time series for the heat flux at the plate stagnation point for different *Re*. The flow regime at the tube outlet: (**a**) laminar—*Re* = 2380, (**b**) transitional—*Re* = 3220, (**c**) turbulent—*Re* = 3790.

In more detail, the relationship between the flow parameters in the initial section of the jet and at the frontal point of the plate at distance h/d = 20 can be observed in Figure 3. Here is a time series for the instantaneous value of the heat flux density q at the plate stagnation point for different Re. So, in Figure 5a for Re = 2372, the instantaneous value of the heat flux density fluctuates near Q = 16,000 W/m^2 with small dispersion without large fluctuations. Velocity measurements at the tube outlet showed that this corresponds to a laminar flow in the tube. Large-scale turbulent structures of the puff type are not formed inside the tube in this regime (γ = 0– intermittency factor). The next oscillogram in Figure 5b at Re = 3320 shows strong fluctuations in the heat flux density. This regime corresponds to the flow when puff-type vortices are formed in the tube. Each formation of a puff in the jet reduces sharply the heat flux at the frontal point of the plate. Thus, this Reynolds number corresponds to the extremum of velocity and heat flux fluctuations. The intermittency coefficient, in this case, is approximately γ = 0.5. That is, statistically, the laminar phase in the tube (without puff) takes half the time, and by the turbulent phase (puff) it takes another half. At Re = 3700 (Figure 5c), a decrease in the average value of the heat flux q stops. The level of q fluctuations also decreases and reaches an approximately constant low value. For this regime, the intermittency coefficient is γ = 1, this means that there is no laminar phase in the tube. With a further increase in the Reynolds number Re > 3700, a pattern does not change, that is, corresponding to a developed turbulent flow

in the tube. Thus, there is an unambiguous relationship between the flow at the tube outlet and the behavior of heat transfer at the stagnation point of the plate. If a laminar-turbulent transition occurs in the tube, which is characterized by a regime with intermittency, then an intermittent nature of the heat flow behavior is also recorded at the plate stagnation point. At that, each appearance of the turbulent puff structure at the tube outlet causes a sharp decrease in the heat flux density on the plate. At the same time, the laminar phase of the flow in the tube causes its sharp increase.

For the first time, heat transfer in an impact jet flowing from a long tube was considered by us in [46,47]. This article presents data on the instantaneous values of the heat flux for three flow regimes in a tube: laminar, transitional and turbulent. In the range of Reynolds numbers characteristic of a laminar-turbulent transition in a tube, the heat flux at the stagnation point noticeably decreases. That is, the heat transfer in the laminar regime is significantly higher than in the turbulent one. This effect is explained by the fact that the laminar jet expands with a small angle of 3–5°, while the turbulent jet has an expansion angle of 20–24° As a result, the heat flow in the laminar regime is distributed over a much smaller area than in the turbulent one. With a further increase in the Reynolds number ($Re > 3700$), an increase in heat transfer is observed, which corresponds to the literature data typical for impact jets flowing from profiled nozzles [48].

6. Interaction of an Impinging Hydrogen Jet with a Catalyst Surface

The next part of the research deals with the interaction of a hydrogen jet with a flat surface of a heated catalyst. Before the gas mixture supply, the catalyst was heated by a heater to a temperature when the effect of an exothermic reaction was recorded. The thermogram of the catalytic surface when H_2/N_2 jet with a hydrogen volume content of 15% flows out of a long tube with an inner diameter of 3 mm onto this surface at an angle of 10 degrees from the normal is presented in Figure 6. In the experiments, a FLIR x650sc thermal imager was used. Figure 6 shows a sample of consecutive frames 1, 2, 3 and 4 received at a frequency of 100 Hz. The green area highlights the zone of heat release as a result of a heterogeneous reaction. A colder spot is observed in the region of the critical point. In the regime of puff structure formation in the jet flow, the temperature field on the surface becomes much more uniform. It should be noted that in the regime of jet source excitation, intensification or, conversely, a decrease in the intensity of heat and mass transfer on the surface depends on the h ratio between the distance from the obstacle and the length of the initial section of the jet and depends significantly on the fuel mixture composition.

In the experiment with a reacting gas and a catalytic surface, it is important to know the relationship between hydrodynamic and chemical processes on the catalyst surface. Unfortunately, due to the complex composition of the catalyst $2\%Pd/10\%CeO_{0.4}ZrO_{0.4}LaO_{0.2}/Al_2O_3$, it is difficult to predict theoretically the chemical reaction constants, and there are no publications concerning the research with catalysts of this composition. As is shown by our methodical experiments using a FLIR x650sc high-speed thermal imager (maximum frequency of 1.5 kHz), if a high-frequency velocity perturbation (~1 kHz) is artificially introduced into the jet flow, then a temperature change with the same frequency is recorded on the catalytic surface. Thus, it has been established that a catalytic palladium-based coating with a thickness of 60 μm deposited on a steel plate with a thickness of 3 mm has low "thermochemical" inertia. That is, the characteristic time of chemical kinetics is much less than the rates of convective processes in the impinging jet near the catalyst wall. This circumstance allows us to estimate with confidence the temperature fluctuations on the plate surface using a thermal imager at various stages of development of the laminar-turbulent transition in the jet flow.

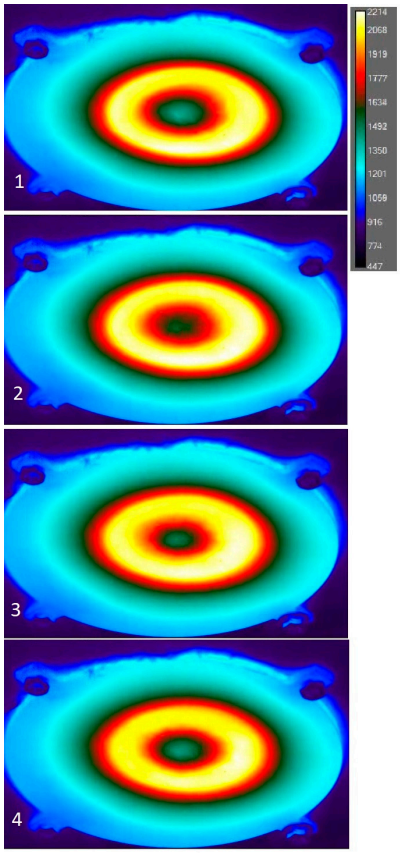

Figure 6. Thermograms of the surface during a heterogeneous reaction of hydrogen oxidation when an H_2/N_2 jet (X_{H2} = 15%) flows onto a catalytically active flat wall. Thermograms, frequency of 100 Hz, d = 5 mm, h/d = 10, Re = 2600.

In this work, the catalyst surface temperature was statistically processed; as a result, thermal fluctuations were determined. For statistics, N = 40 thermograms, measured with a TESTO 890 thermal imager for about 300 s, were used. Each thermogram includes the entire surface of the catalyst. The value of root-mean-square temperature fluctuations was used as a parameter characterizing the intensity of thermal fluctuations in accordance with the formula:

$$T'(r) = \sqrt{\frac{1}{N-1}\sum_{i=1}^{N}(T_i(r) - T_0(r))^2}$$

Here, i is the current thermogram number, $i = 1 \ldots N$, $T_i(r)$ is the temperature at radius r for the i-th thermogram, $T_0(r)$- is the average temperature at radius r. Expression $T_1 = T'(r)/T_{0L}(r)$ is used for normalization, where T_{0L}(r) is the average temperature distribution along the radius in the laminar regime of the jet flow on the obstacle at Re = 1820. Thus, we compare the level of thermal fluctuations in the reacting jet with turbulent large-scale vortices with the flow in the laminar reacting jet without such powerful high-energy structures.

Data on the distribution of dimensionless pulsation of the catalyst surface temperature along the disk radius at h/d = 10 are shown in Figure 7. Figure 7a illustrates the laminar flow; other figures (Figure 7b–f) correspond to the regime of laminar-turbulent transition in the tube. It was experimentally found that in the range of Reynolds numbers Re = 2100–2500 in the tube, and accordingly, in the near region of the impinging jet, the large-scale puff structures are recorded. As it is known, in the regime of laminar-turbulent transition in a tube, the intermittency parameter γ (the ratio of turbulent and laminar sections of the flow) changes in the range γ = 0–1. Based on the data presented in Figure 7b–f, it can be seen that in the case of puff formation, significant temperature fluctuations are observed in the

region of the entire catalyst ($r/d = 0 \ldots +/-15$). At that, the range of normalized thermal fluctuations is from 0.5% to 11% as compared to the laminar flow. It can be also seen that the Reynolds number and, accordingly, the intermittency parameter has a significant effect both on the level of temperature fluctuations and on the nature of its distribution along the radius. Thus, for the case of Re = 2120 (Figure 7b), two temperature fluctuation maxima are observed. The largest extremum is 3.5% and it is located in the region of the critical point. The second local maximum of fluctuations at r/d = 5 is apparently associated with the flow of an impinging jet onto the obstacle of the mixing layer. This character of distribution of fluctuations of thermal parameters with two extrema is similar to the case of an impinging unreacting jet flowing out of confusers at high Reynolds numbers and small distances to the obstacle [49].

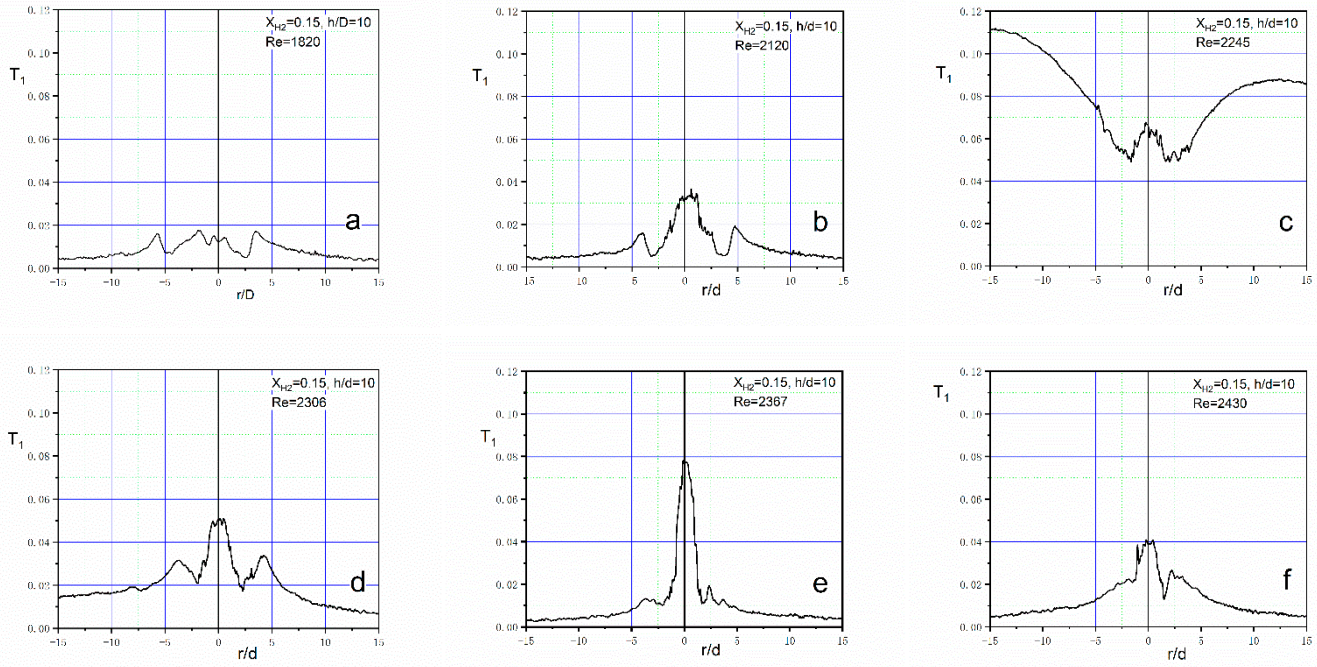

Figure 7. The intensity of temperature fluctuations during the flow of an impingement jet on the catalytic surface (d = 3 mm, h/d = 10, H_2/N_2, X_{H2} = 15%). (**a**)—Re = 1820; (**b**)—Re = 2120; (**c**)—Re = 2245; (**d**)—Re = 2306; (**e**)—Re = 2387; (**f**)—Re = 2430.

With a further increase in the Reynolds number of the fuel jet, the thermal pattern changes non-linearly. At Re = 2245 (Figure 7c), large-scale vortex structures flowing onto the obstacle perturb the entire flow above the plate. This leads to the fact that the level of pulsations at the periphery ($r/d = +/-15$) becomes greater than at the jet axis. At that, the local extremum at the stagnation point is preserved. This is the regime with the maximum integral effect of increasing the temperature fluctuations over the entire area of the catalyst. This mode occurred only at Re = 2245. According to the authors, this effect can be explained using the visualization presented in Figure 3b,c. The large-scale puff structure, when interacting with the wall, transforms into smaller vortices that propagate along the wall. The data presented in Figure 7c were fixed at Reynolds number Re = 2245, which roughly corresponds to the intermittency parameter γ~0.5. In this case, about half the time puff is present in the jet, and the other half of the time puff is absent. In this case, one must keep in mind the statistically random nature of the appearance of puff in a jet source. Further studies are required to confirm the mechanism of this effect more substantiated.

With a further increase to Re = 2306 (Figure 7d), the frequency of puff structure occurrence increases, and the nature of thermal parameter distribution is similar to the case at Re = 2120, i.e., the distribution with two maxima, but with a higher level of fluctuations. The next Reynolds number Re = 2387 (Figure 7e) leads to significant localization of the main

impact in the region of the critical point. At this point, an extremum of thermal fluctuations is reached, which is 8% for the entire range of the laminar-turbulent transition. For the case of the flow closest to the turbulent regime (Re = 2430), the intermittency parameter is γ = 0.95 (Figure 7f). There is also a two-hump distribution with a fluctuation level of 0.5% at the periphery (r/d = +/−15) and 4% in the region of the stagnation point. With a further increase in the Reynolds number (6000 > Re > 2500), the flow regime in the jet source becomes turbulent. For this case, the distribution of fluctuations over the catalyst surface radius remains with two maxima, while the level of temperature fluctuations increases monotonically with increasing Re.

An analysis of data presented in Figure 7 indicates that the presence of large-scale puff structures in the near region of the reacting jet contributes to the occurrence of significant temperature fluctuations in the region of the entire catalyst (r/d = 0 . . . +/−15). With an increase in the Reynolds number, several versions of the distribution of thermal fluctuations over the catalyst area are observed. For practical purposes, two of them should be noted: the first is with maximum temperature fluctuations in the local region of the stagnation point (Figure 7e), and the second is with the largest integral increase in fluctuations over the entire catalyst area (Figure 7c).

It seems interesting to compare thermal fluctuations for three flow regimes in a jet source: laminar, transitional, and turbulent. As it follows from Figure 7b–f, the range of normalized thermal fluctuations in the transient regime is from 0.5% to 11% as compared to the laminar flow regime (Figure 7a). That is, the level of temperature fluctuations in the transient regime is almost always higher than in the laminar regime. Comparison of the transitional regime with the turbulent one (Re < 6000) demonstrates the fact that in the first case there are Reynolds numbers (in the range Re = 2100 – 2500) at which the higher values of temperature fluctuations can be obtained, both in the region of the stagnation point and throughout the catalyst area.

Thus, in the region of the laminar-turbulent transition in the impinging jet, one can obtain a greater intensity of fluctuations on the catalytic surface than for the turbulent flow at low Reynolds numbers (Re < 6000). This result is similar to the effect obtained for heat transfer in an impinging inert gas jet [46]. In this experiment, for a long tube at transitional Reynolds numbers, heat flux fluctuations at the stagnation point are more intense than those for a turbulent flow.

7. Discussion

Previous works devoted to catalytic combustion in impact jets of various gases have shown the existence of different regimes for combining homogeneous and heterogeneous reactions [16]. As is known, in practice, the regime of heterogeneous reactions corresponds to low temperatures of the catalyst surface, as well as a low content of fuel mixed with other gases [50]. This article is devoted to experiments when the reaction was carried out on the surface of the catalyst.

To control the transport processes in impacting reacting jets, we used an approach associated with the use of large-scale vortex structures. This principle is quite well known for intensifying transport processes, for example, in gas-phase flames [21,37,51] and in impact jets [38]. In such flows, the mechanism of hydrodynamic instability in the mixing layer is used to generate large eddies. In this case, the size of coherent structures is l = 2–3 d. Another feature of such flows is high Reynolds numbers (Re > 5000) and profiled nozzles as a jet source. A feature of our work is the use of long round tubes (L > 100 d) and low Re = 2000–4000 numbers when a laminar-turbulent transition occurs in such a channel according to the intermittency scenario [32]. Previously, we [40] have shown that in this case, it is possible to obtain superstructures with a size of l = 20–30 d with a high level of velocity fluctuations. When using our approach to intensify heat transfer in impact jets, it is possible to use a working gas with a lower flow rate, since the range of Reynolds numbers is significant [46,47]. In this work, we tried to develop this approach in relation to the impingement of a hydrogen jet on a flat catalyst surface.

At the beginning of this work, we performed the visualization of puff in an impact jet of Freon F-22 using the Schlieren method of Hilbert optics for the distance from the beginning of the jet to the surface h/d = 10. This working gas was chosen to obtain maximum contrast when visualizing the flow. The mechanism of puff formation in a long tube does not depend on the type of gas but is determined by the Reynolds number and initial conditions [40]. It was shown that the near zone of the jet contains large-scale puff-type vortex structures. In the region of the critical point, large-scale structures are strongly deformed. As a result, its longitudinal size is apparently reduced, and the superstructure is transformed into smaller vortices that propagate along the wall. In this work, the process of vortex dynamics in the near-wall flow region was not studied. It would be interesting to compare it with the classical problem of the interaction of a single vortex with a wall [52].

However, the minimum number Re_1, at which puff occurs and, accordingly, the intermittency coefficient becomes different from zero, as well as Re_2, when $\gamma = 1$, that is, turbulent flow sets in, differ for our different experiments. This is explained by the fact that the critical Reynolds number for flow in pipes depends on many parameters, including Re_1, which is sensitive to the level of initial disturbances [32]. The limiting number reported in the literature is $Re_1 = 10^5$ [32]. In our experiments, flexible gas supply lines (from the gas source to the tube inlet) of various designs were used, while the level of perturbations at the tube inlet was not controlled.

The internal structure of puff vortices was studied using high-speed PIV in a free CO_2 jet. The velocity field was studied within a single puff with a time resolution corresponding to the frequency f = 7 kHz. It was found that the correlation of the instantaneous value of the velocity at different radii characterizes the transverse size of puff, which is 2–4 d. However, the longitudinal size of the vortices in the jet varies within 20–30 d, which slightly exceeds the puff size of 10–20 d obtained in long channels with a circular cross-section [32,33].

The next stage of our work was devoted to the study of the heat flux density at the critical point of an impact air jet using a film sensor with a high time resolution (up to 3 kHz). As a result, an unambiguous relationship was established between the parameters in the initial section of the jet and at the plate stagnation point. If a laminar-turbulent transition occurs in the pipe, which is characterized by a regime with intermittency, then an intermittent nature of the heat flow behavior is also recorded at the plate stagnation point. In this case, each appearance of the turbulent puff structure at the tube outlet causes a sharp decrease in the heat flux density on the plate. At the same time, the laminar phase of the flow in the pipe causes its sharp increase. Such data on heat flux fluctuations at low Reynolds numbers were obtained for the first time and differ from the results obtained in impact jets at high Reynolds numbers [49].

The final task in this work was to study temperature fluctuations on the catalyst surface in an $H_2 + N_2$ impact jet using a low-speed (Testo890-2) and high-speed (FLIR x6530sc) thermal imager. It has been shown in this work that the interaction of a reacting impact jet of a hydrogen/N_2 mixture with a palladium-based catalyst results in intense temperature fluctuations on the catalyst surface. This effect was obtained at a low hydrogen content in the X_{H2} = 15% mixture and a low catalyst temperature (Tc = 180 °C) under the thermodynamic conditions of ambient air (atmospheric pressure and room temperature). Such experimental conditions correspond to the heterogeneous mechanism of chemical reactions during catalytic combustion [16]. Thermal fluctuations on the catalyst surface are compared at h/d = 10 for three flow regimes in a jet source: laminar, transitional, and turbulent. It is shown that the smallest temperature fluctuations are obtained for the laminar regime (<1.5%), and are more significant (<4%) for the turbulent regime at low Reynolds numbers (Re < 6000). The largest temperature fluctuations were obtained in the regime of laminar-turbulent transition (up to 11%). Based on the distribution of temperature fluctuations over the area of a flat round catalyst, two important regimes were established. The first mode is with maximum temperature fluctuations in the region of the stagnation point, the second mode is with the largest integral increase in temperature fluctuations over the entire catalyst area.

The advantage of the first mode can be used where process localization is required. In particular, inkjet printing in heterogeneous catalysis [53]. The practical significance of the second mode is due, for example, to the fact that the CVD process requires a uniform coating of a solid surface [11]. Local inhomogeneity of the coating thickness, in turn, leads to earlier wear of the protective surfaces. The data presented in the final task was obtained for the first time.

8. Conclusions

This work is aimed at using large-scale turbulent structures in gas flows to intensify the heat and mass transfer processes during the interaction of impact jets with inert and chemically reacting surfaces. In our previous works [39,40,54] a method was developed for generating large-scale turbulent structures in jets by forming them using long tubes ($L/d > 100$) in the laminar-turbulent transition mode. An essential feature of our approach from the traditional method with the generation of coherent structures is the use of low Reynolds numbers and superstructures. In the presented material, when solving the problem of controlling the transfer processes, the following tasks were performed: (a) visualization of the flow in the F-22 impact jet from the point of view of detecting puff structures; (b) studying the internal structure of a single puff using high-speed PIV using the example of a free jet of CO_2; (c) measurement of the instantaneous heat flux on a flat wall for an impact air jet; (d) study of temperature field fluctuations on the catalyst surface for an impact jet of an H_2/N_2 mixture. A distinctive feature of this study is: (a) a low-cost palladium-based catalyst ($2\%Pd/10\%CeO_{0.4}ZrO_{0.4}LaO_{0.2}/Al_2O_3$) and a simple technological method of its application to the surface (Pechini method); (b) low hydrogen content in the mixture gas (X_{H2}/X_{N2} = 15/85%) in an impact jet; (c) low surface temperature of the preheated catalyst (T_C = 180 °C). All experiments were performed under the thermodynamic conditions of ambient air (atmospheric pressure and room temperature). Finally, the following conclusions can be drawn from the work.

1. Thermal fluctuations on the catalyst surface were measured at h/d = 10 for three flow regimes in a jet source: laminar, transitional, and turbulent. It is shown that the smallest temperature fluctuations are obtained for the laminar regime (<1.5%) and are more significant (<4%) for the turbulent regime at low Reynolds numbers (Re < 6000). The maximum temperature fluctuations (up to 11%) were obtained in the laminar-turbulent transition mode at Re = 3100–3700.
2. High-intensity temperature fluctuations on the catalyst surface occur when a jet flows onto the catalyst, which contains large-scale vortex structures—puff (l/d = 20–30).
3. Two important regimes have been established from the point of distribution of temperature fluctuations over the area of a flat round catalyst in the range Re = 3100–3700. The first regime is with maximum temperature fluctuations in the region of the stagnation point, the second regime is with the largest integral increase in temperature fluctuations over the entire catalyst area.

The effect of high-intensity temperature fluctuations on the catalyst surface was obtained at a fixed distance from the beginning of the jet to the catalyst h/d = 10. Previously, we showed [55] that the distance from the nozzle to the point of transition to turbulence in an inert jet depends both on the Reynolds number and on the hydrodynamic conditions at the inlet to a long pipe (channel cross-sectional shape, initial velocity profile, pulsation level speed, etc.). Thus, apparently, the effect obtained on the catalyst may depend on the initial conditions in the jet source. Also, as a continuation of this work, we plan to study homogeneous reactions within the framework of the problem of catalytic combustion. From a practical point of view, the approach using large-scale turbulent structures is promising for the intensification of heat and mass transfer processes during catalytic combustion and catalytic heating, as well as for the intensification of CVD processes.

Author Contributions: Methodology, V.L. (Vadim Lemanov); Investigation, V.L. (Vladimir Lukashov) and K.S.; Resources, V.L. (Vadim Lemanov); Writing—original draft, V.L. (Vadim Lemanov),

V.L. (Vladimir Lukashov) and K.S.; Writing—review & editing, V.L. (Vladimir Lukashov) and K.S. All authors have read and agreed to the published version of the manuscript.

Funding: This research was funded by the Ministry of Science and Higher Education of the Russian Federation, grant number 075-15-2020-806.

Acknowledgments: Eduard Arbuzov provided great assistance to the authors in conducting experiments.

Conflicts of Interest: The authors declare no conflict of interest.

Nomenclature

d	tube diameter, mm
h	distance from tube to obstacle, mm
L	tube length, m
l	large vortex length, m
Q	instantaneous value of heat-flux density, W/m2
r	radial coordinate, mm
$Re = Ud/\nu$	Reynolds number
Re_1	lower boundary of the laminar-turbulent transition
Re_2	top boundary of the laminar-turbulent transition
t	time, s
T	instantaneous value of temperature, °C
T_0	average temperature, °C
T'	temperature pulsations, °C
Tc	catalyst temperature, °C
Tw	wall temperature, °C
T_1	dimensionless temperature
$Tu = u/Um \times 100\%$	turbulence level, %
U	bulk gas velocity in the tube, m/s
Um	axial gas velocity at the tube outlet, m/s
u	root-mean-square of velocity fluctuations, m/s
X	molar fraction
δ	thickness of the boundary layer, mm
x	longitudinal coordinate, mm
γ	intermittency factor

References

1. Kim, J.; Yu, J.; Lee, S.; Tahmasebi, A.; Jeon, C.-H.; Lucas, J. Advances in Catalytic Hydrogen Combustion Research: Catalysts, Mechanism, Kinetics, and Reactor Designs. *Int. J. Hydrogen Energy* **2021**, *46*, 40073–40104. [CrossRef]
2. Mantzaras, J. Progress in Non-Intrusive Laser-Based Measurements of Gas-Phase Thermoscalars and Supporting Modeling near Catalytic Interfaces. *Prog. Energy Combust. Sci.* **2019**, *70*, 169–211. [CrossRef]
3. Johnson, T.A.; Kanouff, M.P. Development of a Hydrogen Catalytic Heater for Heating Metal Hydride Hydrogen Storage Systems. *Int. J. Hydrogen Energy* **2012**, *37*, 2304–2319. [CrossRef]
4. Argyle, M.; Bartholomew, C. Heterogeneous Catalyst Deactivation and Regeneration: A Review. *Catalysts* **2015**, *5*, 145–269. [CrossRef]
5. Chien, Y.-C.; Dunn-Rankin, D. Electric Field Induced Changes of a Diffusion Flame and Heat Transfer near an Impinging Surface. *Energies* **2018**, *11*, 1235. [CrossRef]
6. Rehage, H.; Kind, M. The First Damköhler Number and Its Importance for Characterizing the Influence of Mixing on Competitive Chemical Reactions. *Chem. Eng. Sci.* **2021**, *229*, 116007. [CrossRef]
7. Chiu, C.-P.; Yeh, S.-I.; Tsai, Y.-C.; Yang, J.-T. An Investigation of Fuel Mixing and Reaction in a CH_4/Syngas/Air Premixed Impinging Flame with Varied H_2/CO Proportion. *Energies* **2017**, *10*, 900. [CrossRef]
8. Liu, X.; Yue, S.; Lu, L.; Gao, W.; Li, J. Experimental and Numerical Studies on Flow and Turbulence Characteristics of Impinging Stream Reactors with Dynamic Inlet Velocity Variation. *Energies* **2018**, *11*, 1717. [CrossRef]
9. Karakaya, C.; Deutschmann, O. Kinetics of Hydrogen Oxidation on Rh/Al_2O_3 Catalysts Studied in a Stagnation-Flow Reactor. *Chem. Eng. Sci.* **2013**, *89*, 171–184. [CrossRef]
10. Rubtsov, N.M.; Seplyarskii, B.S.; Alymov, M.I. *Initiation and Flame Propagation in Combustion of Gases and Pyrophoric Metal Nanostructures*; Springer International Publishing: Berlin/Heidelberg, Germany, 2021.
11. Igumenov, I.K.; Lukashov, V.V. Modern Solutions for Functional Coatings in CVD Processes. *Coatings* **2022**, *12*, 1265. [CrossRef]
12. Schlögl, R. Heterogeneous Catalysis. *Angew. Chem. Int. Ed.* **2015**, *54*, 3465–3520. [CrossRef] [PubMed]

13. Imbihl, R. Nonlinear Dynamics on Catalytic Surfaces: The Contribution of Surface Science. *Surf. Sci.* **2009**, *603*, 1671–1679. [CrossRef]
14. Wang, A.; Li, J.; Zhang, T. Heterogeneous Single-Atom Catalysis. *Nat. Rev. Chem.* **2018**, *2*, 65–81. [CrossRef]
15. Imbihl, R.; Behm, R.J.; Schlögl, R. Bridging the Pressure and Material Gap in Heterogeneous Catalysis. *Phys. Chem. Chem. Phys.* **2007**, *9*, 3459. [CrossRef] [PubMed]
16. Ikeda, H.; Libby, P.A.; Williams, F.A.; Sato, J. Catalytic Combustion of Hydrogen-Air Mixtures in Stagnation Flows. *Combust. Flame* **1993**, *93*, 138–148. [CrossRef]
17. Tong, T.W.; Abou-Ellail, M.M.; Li, Y. Mathematical Modeling of Impinging Hydrogen-Air Flows Augmented by Catalytic Surface Reactions. *J. Thermophys. Heat Trans.* **2008**, *22*, 709–717. [CrossRef]
18. Williams, W.R.; Stenzel, M.T.; Song, X.; Schmidt, L.D. Bifurcation Behavior in Homogeneous-Heterogeneous Combustion: I. Experimental Results over Platinum. *Combust. Flame* **1991**, *84*, 277–291. [CrossRef]
19. Ikeda, H.; Sato, J.; Williams, F.A. Surface Kinetics for Catalytic Combustion of Hydrogen-Air Mixtures on Platinum at Atmospheric Pressure in Stagnation Flows. *Surf. Sci.* **1995**, *326*, 11–26. [CrossRef]
20. Sidwell, R.W.; Zhu, H.; Kee, R.J.; Wickham, D.T.; Schell, C.; Jackson, G.S. Catalytic Combustion of Premixed Methane/Air on a Palladium-Substituted Hexaluminate Stagnation Surface. *Proc. Combust. Inst.* **2002**, *29*, 1013–1020. [CrossRef]
21. Renard, P.-H.; Thévenin, D.; Rolon, J.C.; Candel, S. Dynamics of Flame/Vortex Interactions. *Prog. Energy Combust. Sci.* **2000**, *26*, 225–282. [CrossRef]
22. Ginevsky, A.S.; Vlasov, Y.V.; Karavosov, R.K. *Acoustic Control of Turbulent Jets*; Springer: Berlin/Heidelberg, Germany, 2004. [CrossRef]
23. Kline, S.J.; Reynolds, W.C.; Schraub, F.A.; Runstadler, P.W. The Structure of Turbulent Boundary Layers. *J. Fluid Mech.* **1967**, *30*, 741–773. [CrossRef]
24. Brown, G.L.; Roshko, A. On Density Effects and Large Structure in Turbulent Mixing Layers. *J. Fluid Mech.* **1974**, *64*, 775–816. [CrossRef]
25. Kovasznay, L.S.G. Large Scale Structure in Turbulence: A Question or an Answer? In *Structure and Mechanisms of Turbulence I*; Fiedler, H., Ed.; Springer: Berlin/Heidelberg, Germany, 1978; pp. 1–18.
26. Hussain, A.K.M.F. Coherent Structures—Reality and Myth. *Phys. Fluids* **1983**, *26*, 2816. [CrossRef]
27. Fiedler, H.E. Coherent Structures in Turbulent Flows. *Prog. Aerosp. Sci.* **1988**, *25*, 231–269. [CrossRef]
28. Cantwell, B. Future Directions in Turbulence Research and the Role of Organized Motion. In *Whither Turbulence? Turbulence at the CrossroadsI*; Springer: Berlin/Heidelberg, Germany, 2005; pp. 97–131. [CrossRef]
29. Guala, M.; Hommema, S.E.; Adrian, R.J. Large-Scale and Very-Large-Scale Motions in Turbulent Pipe Flow. *J. Fluid Mech.* **2006**, *554*, 521. [CrossRef]
30. Hutchins, N.; Marusic, I. Evidence of Very Long Meandering Features in the Logarithmic Region of Turbulent Boundary Layers. *J. Fluid Mech.* **2007**, *579*, 1–28. [CrossRef]
31. Schumacher, J.; Eckhardt, B.; Haller, G. Turbulent superstructures in closed and open flows. In Proceedings of the Euromech Colloquium 586, Erfurt, Germany, 12–14 July 2017.
32. Mullin, T. Experimental Studies of Transition to Turbulence in a Pipe. *Annu. Rev. Fluid Mech.* **2011**, *43*, 1–24. [CrossRef]
33. Wygnanski, I.J.; Champagne, F.H. On Transition in a Pipe. Part 1. The Origin of Puffs and Slugs and the Flow in a Turbulent Slug. *J. Fluid Mech.* **1973**, *59*, 281–335. [CrossRef]
34. Avila, K.; Moxey, D.; de Lozar, A.; Avila, M.; Barkley, D.; Hof, B. The Onset of Turbulence in Pipe Flow. *Science* **2011**, *333*, 192–196. [CrossRef]
35. Borghi, R.; Murthy, S.N. *Turbulent Reactive Flows*; Springer: New York, NY, USA, 1989.
36. Liñán, A.; Vera, M.; Sánchez, A.L. Ignition, Liftoff, and Extinction of Gaseous Diffusion Flames. *Annu. Rev. Fluid Mech.* **2015**, *47*, 293–314. [CrossRef]
37. Rajasegar, R.; Choi, J.; McGann, B.; Oldani, A.; Lee, T.; Hammack, S.D.; Carter, C.D.; Yoo, J. Comprehensive Combustion Stability Analysis Using Dynamic Mode Decomposition. *Energy Fuels* **2018**, *32*, 9990–9996. [CrossRef]
38. Jin, L.; Cao, Y. Coherent Structures and Mixing Enhancement in a Confined Impinging-Jet Mixer. *Chem. Eng. Sci.* **2022**, *262*, 118014. [CrossRef]
39. Lemanov, V.V.; Lukashov, V.V.; Sharov, K.A. Transition to Turbulence through Intermittence in Inert and Reacting Jets. *Fluid Dyn.* **2020**, *55*, 768–777. [CrossRef]
40. Lemanov, V.; Lukashov, V.; Sharov, K. Turbulent Superstructures in Inert Jets and Diffusion Jet Flames. *Fluids* **2021**, *6*, 459. [CrossRef]
41. Vargaftik, N.B. *Tables on the Thermophysical Properties of Liquids and Gases*, 2nd ed.; John Wiley & Sons, Inc.: New York, NY, USA, 1975.
42. Laberty-Robert, C.; Ansart, F.; Deloget, C.; Gaudon, M.; Rousset, A. Dense Yttria Stabilized Zirconia: Sintering and Microstructure. *Ceram. Int.* **2003**, *29*, 151–158. [CrossRef]
43. Mityakov, A.V.; Sapozhnikov, S.Z.; Mityakov, V.Y.; Snarskii, A.A.; Zhenirovsky, M.I.; Pyrhönen, J.J. Gradient Heat Flux Sensors for High Temperature Environments. *Sens. Actuators A Phys.* **2012**, *176*, 1–9. [CrossRef]
44. Akhmetbekov, Y.K.; Bilsky, A.V.; Lozhkin, Y.A.; Markovich, D.M.; Tokarev, M.P.; Tyuryushkin, A.N. Software for Experiment Management and Processing of Data Obtained by Digital Flow Visualization Techniques (ActualFlow). *Num. Meth. Prog* **2006**, *73*, 79–85. (In Russian)

45. Nikolaevich, D.Y.; Vladimirovich, L.V.; Vladimirovich, L.V.; Anisiforovich, A.V.; Aleksandrovich, S.K. Hydrodynamic Vortex Structures in a Diffusion Jet Flame. In *Swirling Flows and Flames*; Boushaki, T., Ed.; IntechOpen: Rijeka, Croatia, 2018.
46. Lemanov, V.V.; Terekhov, V.I. Specific Features of Heat Transfer at the Stagnation Point of an Impact Axisymmetric Jet at Low Reynolds Numbers. *High Temp.* **2016**, *54*, 454–456. [CrossRef]
47. Lemanov, V.; Matyunin, V.; Travnicek, Z. Heat Transfer at the Stagnation Point of the Impinging Laminar Jet. *J. Phys. Conf. Ser.* **2020**, *1677*, 12018. [CrossRef]
48. Zuckerman, N.; Lior, N. Jet Impingement Heat Transfer: Physics, Correlations, and Numerical Modeling. *Adv. Heat Transf.* **2006**, *39*, 565–631. [CrossRef]
49. Liu, T.; Sullivan, J.P. Heat Transfer and Flow Structures in an Excited Circular Impinging Jet. *Int. J. Heat Mass Transf.* **1996**, *39*, 3695–3706. [CrossRef]
50. Mantzaras, J. Catalytic Combustion of Hydrogen, Challenges, and Opportunities. *Adv. Chem. Eng.* **2014**, *45*, 97–157. [CrossRef]
51. Huang, Y.; Yang, V. Dynamics and Stability of Lean-Premixed Swirl-Stabilized Combustion. *Prog. Energy Combust. Sci.* **2009**, *35*, 293–364. [CrossRef]
52. Doligalski, T.L.; Smith, C.R.; Walker, J.D.A. Vortex Interactions with Walls. *Annu. Rev. Fluid Mech.* **1994**, *26*, 573–616. [CrossRef]
53. Maleki, H.; Bertola, V. Recent Advances and Prospects of Inkjet Printing in Heterogeneous Catalysis. *Catal. Sci. Technol.* **2020**, *10*, 3140–3159. [CrossRef]
54. Lemanov, V.V.; Lukashov, V.V.; Abdrakhmanov, R.; Arbuzov, V.A.; Dubnishchev, Y.N.; Sharov, K.A. Regimes of Unstable Expansion and Diffusion Combustion of a Hydrocarbon Fuel Jet. *Combust. Explos. Shock Waves* **2018**, *54*, 255–263. [CrossRef]
55. Lemanov, V.V.; Terekhov, V.I.; Sharov, K.A.; Shumeiko, A.A. An Experimental Study of Submerged Jets at Low Reynolds Numbers. *Tech. Phys. Lett.* **2013**, *39*, 421–423. [CrossRef]